

## LETTER TO THE EDITOR

**Dominance of short-range correlations in photoejection-induced excitation processes**Kurt W Meyer<sup>†</sup>, John L Bohn<sup>‡</sup>, Chris H Greene<sup>†§</sup> and Brett D Esry<sup>†</sup><sup>†</sup> Department of Physics and JILA, University of Colorado, Boulder, CO 80309-0440, USA<sup>‡</sup> Quantum Physics Division, NIST, Boulder, CO 80309, USA

Received 5 August 1997

**Abstract.** Much attention has been focused in recent decades on the process of double photoejection, with comparatively little study of the closely related process of photoejection plus excitation of the residual fragment. We present new calculations for the process  $h\nu + \text{He} \rightarrow \text{He}^+(n) + e^-$ , which quantitatively reproduces recent experimental measurements (Wehlitz *et al* 1997 *J. Phys. B: At. Mol. Opt. Phys.* **30** L51). These calculations show that the controlling electron correlations are confined to distances much smaller than the extent ( $\sim 3n^2/Z$  au) of the  $\text{He}^+(n)$  state that is excited.

Several outcomes are possible when a two-electron atom or ion absorbs a photon with an energy large enough to eject both electrons. One electron can absorb all of the photon's energy, leaving the remaining electron in a 1s state. This is observed to be the most likely possibility for helium, and would in fact be the only possible process if all electron–electron interactions were neglected. Different processes can occur if one electron absorbs all of the photon's energy, but exchanges energy with the other electron as it attempts to leave the atom. (This energy exchange is in contrast to ‘shake-off’-type approximations, which neglect final-state correlations.) If the energy-sharing process is such that both electrons possess enough energy to leave the atom, then double escape can occur (double photoejection). Conversely, one electron may not receive enough energy to escape the atom, but will be able to reach higher  $n$  states, a process we will denote as photoejection-induced excitation (PIE) (a small contribution to these processes also occurs due to electron–electron interactions in the ground state). The quantitative description of this latter process is the subject of this letter. In particular, we present theoretical evidence that the ‘decision’ as to which set of principal quanta  $n$  will be excited in a PIE process is made at surprisingly short distances  $r_0 \ll 3n^2/Z$  au, the extent of the  $\text{He}^+(n)$  state. That is, information extracted from a short-range calculation ( $r < r_0$ ) correctly apportions energy between a residual fragment much larger than  $r_0$  and an escaping electron.

Although there has been much focus on the ratio of double to single photoejection in characterizing the strength of electron–electron interactions, the role of these interactions in PIE have been somewhat neglected. Previous experimental and theoretical attempts to determine PIE cross sections in helium have recently been summarized by Wehlitz *et al* [1]. In addition, Wehlitz *et al* have published experimental values for the intensity of helium

§ E-mail address: chg@jilacg.colorado.edu

satellites  $\text{He}^+(n)$  ( $n = 2-6$ ) relative to the main ( $n = 1$ ) line over a wide range of photon energies above the double-escape threshold. Previous studies had focused primarily on the low satellite states ( $n \leq 3$ ) over a limited range of photon energies. Various studies have also addressed the closely related problem of target excitation by electron impact for e-H [2], e- $\text{He}^+$  [3] and e-He [4] scattering.

The use of finite-range pseudostates [5, 6] has been shown to permit an approximate description of the two-electron continuum within an enlarged view of the close-coupling framework [7]. Yet the expectation of traditional close-coupling theory has remained, namely that excitation of a high-lying bound state of principal quantum number  $n$  requires the use of a basis set whose spatial extent encompasses the size of that entire hydrogenic eigenstate. The theoretical development below shows that this view is too pessimistic: it is possible to describe the excitation of  $\text{He}^+(n)$  using a surprisingly compact variational basis set.

In this study, we combine the eigenchannel  $R$ -matrix method with a finite-element approach to address PIE processes. The starting point of this method (see figure 1) is the generation of a set of eigenstates  $\phi_{\bar{n}}$  of the target-state Hamiltonian in a *shrunk* configuration space. Virtually all methods used currently utilize some such set of shrunk eigenstates. The  $R$ -matrix scheme adopted here confines the target states to  $0 < r < r_0$  by simply limiting the Hilbert space to those functions that vanish at  $r = r_0$ . Other methods (e.g. convergent close coupling) produce a shrinkage by using a finite discretized basis set

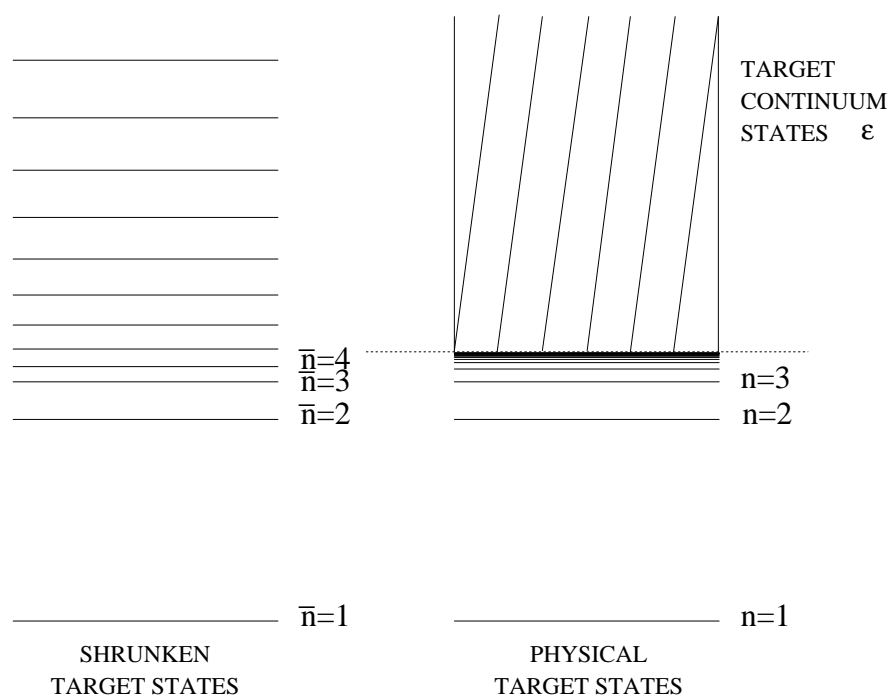


**Figure 1.** Comparison of the energy spectra of the eigenstates of the physical target-state Hamiltonian with the eigenstates of the target-state Hamiltonian in a shrunk configuration space. The physical target states consist of a Rydberg series and an infinite set of continuum states of energy  $\epsilon$ , whereas only discrete states appear for the spectrum in the shrunk space. Note the good correspondence in energies for the lowest few states, as these physical states fit within the shrunk configuration space.

each of the additional members of which extend to successively larger radii. Hyperspherical studies [8] obtain a discrete representation by converting the ratio of the inner and outer electron radial coordinates into an angle with a finite range.

All methods, including ours, solve the time-independent Schrödinger equation by an expansion into this basis set, either explicitly or implicitly. We obtain our initial state, which fits within the shrunken configuration space, by simply diagonalizing the Hamiltonian matrix (including ‘all’ electron–electron correlation effects), formed using a two-electron finite-element basis set consisting of elements which vanish on the surface of the reaction volume.

In contrast to the initial state, the final-state wavefunction is a solution of the Schrödinger equation for specific total energy  $E$ , the sum of the initial state and photon energies. After rearranging the Rayleigh–Ritz variational principle for a specified energy and imposing the eigenchannel  $R$ -matrix choice that the logarithmic derivative of the wavefunction is constant over the surface of a finite reaction volume [9], we obtain a generalized eigensystem. Our choice of basis set is an expanded version of the basis set used to obtain the initial state. In addition to finite elements which vanish at  $r = r_0$ , we include products of one-electron target eigenstates that vanish at  $r = r_0$  with a one-electron finite basis function that is *non-vanishing* at  $r = r_0$ . This addition to our basis set is necessary for describing a final-state wavefunction which is non-zero on the surface of the reaction volume. By solving for the eigenvalues of a generalized eigensystem, we obtain a set of independent solutions equal in number to the number of open or weakly closed channels included in our calculation (the latter are energetically forbidden at larger radial distances, but still participate in the short-range physics).

We have previously applied this method to treat two-electron photoejection processes [10, 11]. In addressing two-electron escape, one might suspect that we include products of *two* non-vanishing one-electron basis functions for our final-state basis set. However, this is not the case. Inclusion of such product-type basis functions would require a two-particle matching scheme with a wavefunction representing the motion of the two electrons outside of the reaction volume. The determination of an exact analytical expression for the three-body Coulomb continuum wavefunction remains an unsolved problem [12]. By selecting product basis functions in which the radial coordinate of at least one electron is zero on the surface of the reaction volume, we are able to employ the same one-electron matching scheme used for describing single-electron escape.

Our choice of basis set also allows us to distinguish between an ‘inner’ electron and an ‘outer’ electron, at least in the region outside the reaction volume. There we make the approximation that the inner electron effectively shields the nucleus, leaving the outer electron in a Coulomb potential of charge  $Z - 1$ , where  $Z$  is the nuclear charge. Inherent in this approximation is the assumption of an unequal energy distribution between the two escaping electrons; that is, one electron receives most of the photon’s energy and quickly leaves the atom (with excess energy  $E_1$ ). The remaining electron is temporarily left near the nucleus before eventually escaping (with excess energy  $E_2$ ). At energies just above threshold, double-escape events are known to occur with equal probabilities for all possible values of  $E_1/E_2$  [13]; therefore, our approximation is poorest for this energy range. Already, at a few eV above threshold, however, experiment has shown [14] that double escape is dominated by unequal energy sharing processes. For this reason, we have confidence that our method will give accurate results for all energies except within a few eV of threshold.

An important issue for our approach is the interpretation of the eigenstates representing the ‘inner’ electron. Since these states are eigenstates of the target Hamiltonian that only span a shrunken configuration space, it is natural to ask how this method can describe two-

electron escape or single-electron escape with the remaining electron excited to a hydrogenic state that ranges outside our box. We view the inner electron pseudostates (target eigenstates in a shrunken configuration space) as simply representing a convenient intermediate basis set that ‘discretizes the continuum’. Ultimately, in order to describe real observables, we must express our results in terms of physical target eigenstates (see figure 1). Although the one-electron pseudostates form a complete set in the shrunken Hilbert space, we can also view these functions as belonging to the entire Hilbert space, being defined as identically zero for  $r \geq r_0$ . Each of these pseudostate functions can then be projected out onto a complete set of states spanning the entire Hilbert space, namely the infinite discrete set of bound target eigenstates  $n = 1, 2, 3, \dots$  and the uncountable infinity of target continuum states of positive energy  $\epsilon$ .

The projection method we have adopted (referred to in [15] as a frame transformation) was used previously to relate pseudostate excitation cross sections to ionization cross sections in electron scattering [15] and to double-escape cross sections in electron photoejection processes [11]. The total double-escape cross section is constructed by summing over the projections of the pseudostate probability amplitudes onto the physical hydrogenic continuum states of energy  $\epsilon$ , then integrating the squared amplitude over the continuum state energy for  $0 \leq \epsilon \leq E$ . The photoejection cross section is given (in au) by

$$\sigma = 4\pi^2\alpha\omega \sum_l \int_0^E d\epsilon \left| \sum_{\bar{n}\bar{l}} \langle \epsilon l | \bar{n}\bar{l} \rangle D_{\bar{n}\bar{l},g}^{(-)\text{box}} \right|^2 \quad (1)$$

where  $D_{\bar{n}\bar{l},g}^{(-)\text{box}}$  represents the length form of the dipole matrix element for excitation of the inner electron from the ground state ‘ $g$ ’ to the final pseudostate  $\bar{n}\bar{l}$ ,  $\alpha$  is the fine-structure constant and  $\omega$  is the photon energy in au. In order to obtain cross sections for PIE we project the inner electron pseudostates onto bound hydrogenic target states; that is, the box dipole matrix elements  $D^{(-)\text{box}}$  are related to the physical dipole matrix elements  $D^{(-)\text{phys}}$  by

$$D_{nl,g}^{(-)\text{phys}} = \sum_{\bar{n}\bar{l}} \langle nl | \bar{n}\bar{l} \rangle D_{\bar{n}\bar{l},g}^{(-)\text{box}} \quad (2)$$

where  $\bar{n}\bar{l}$  label final pseudostates corresponding to the inner electron,  $nl$  label the final bound target eigenstates and  $g$  refers to the two-electron ground state. This frame transformation technique is used to obtain the results shown below.

The low- $n$  target states ( $n = 1, 2, 3$ ) fit within our  $R$ -matrix box. The energies of the eigenstates  $\phi_{\bar{n}}$  of the target-state Hamiltonian in the shrunken configuration space therefore correspond closely to the energies of the physical target state for these low- $n$  values (see figure 1). Consequently, the frame transformation technique (equation (2)) is not required for calculating accurate PIE cross sections for these states. For excitation to higher  $n$  states, the physical target states are represented by the set of pseudostates confined to our  $R$ -matrix box. A simple picture of the remaining electron being in a high Rydberg state indicates that it has a large probability of ‘being located’ outside our reaction volume, the region where our simplified assumption of electron–electron interactions is imposed. For this reason, one expects that only a method which could accurately represent electron–electron correlations out to large distances (large enough to contain the inner electron wavefunction) would be capable of accurately describing excitation to high- $n$  states. However, a previous application of our method to describe helium double photoejection gave reasonable results [11]. This application involved the projection of our pseudostates onto the physical continuum eigenstates which extended out to infinity. Therefore, it should

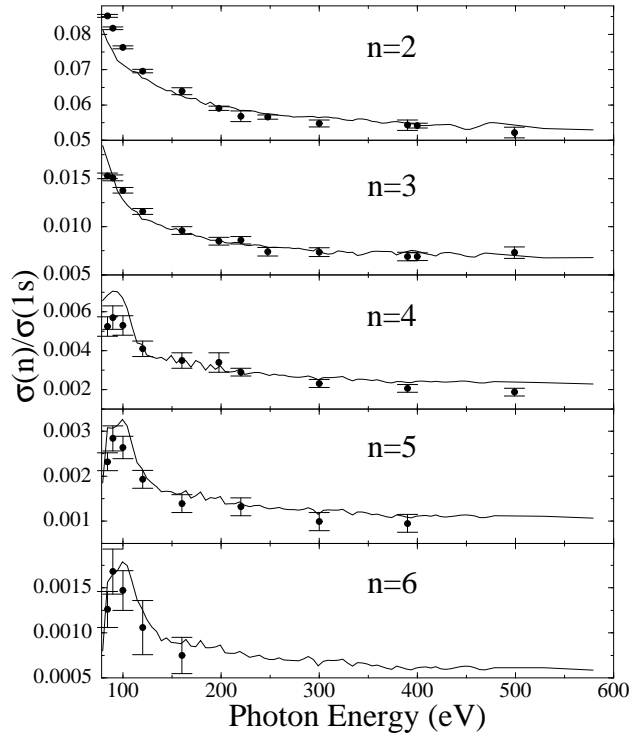


**Figure 2.**  $\sigma_n/\sigma_{1s}$  branching ratios for  $n = 2-6$ . The curves are our calculated eigenchannel  $R$ -matrix values, while the circles are the experimental values of Wehlitz *et al* [1].

not be totally unexpected that this method can also describe excitation to high-lying bound states which extend beyond our  $R$ -matrix box.

The comparison of our  $\sigma_n/\sigma_{1s}$  branching ratios with the experimental values of Wehlitz *et al* [1] is shown in figure 2. Our results for the first 200 eV above threshold were obtained by averaging over five box sizes in the range 12–16 au, while results at higher energies were obtained with a single box size of 10 au. A smaller reaction volume can be used at higher energies since electron correlations are more tightly confined near the nucleus. Gailitis averaging, as described in [10], was used to further improve the stability of the calculation. Photoionization with the remaining electron left in a  $1s$  state accounts for roughly 90% of the total single-ionization cross section in helium. Our ratios for  $n = 2$  and  $n = 3$  agree well with the experimental values across an energy range from the double-escape threshold (78.98 eV) up to 500 eV, although a few of our calculated values lie slightly outside the experimental error bars. Remarkably, this good agreement also holds for  $n = 4-6$ , even though these states extend beyond our  $R$ -matrix box. This indicates that long-range correlations between electrons have little effect on the electron energy distribution for PIE processes to high- $n$  states; that is, the ‘decision’ of the inner electron to be excited to a higher  $n$  state is made while the electron is still near the nucleus.

Although the experiment of Wehlitz *et al* was only capable of measuring cross section ratios, they extracted absolute cross sections by using the total cross section measurements from Samson *et al* [16]. Our  $n = 1$  absolute cross sections lie within the error bars of Wehlitz *et al* over the entire energy range. The single-ionization cross section of helium-like systems decreases [17] as  $E^{-7/2}$  at high (but non-relativistic) energies. Our calculated partial cross

sections are found to decrease at a slightly faster rate at high photon energies, indicating that the limiting  $E^{-7/2}$  dependence has not yet been attained. Partial cross sections for helium are found to scale as  $1/n^3$  for  $n \geq 3$ , a consequence of the  $1/n^3$  frequency scale of Rydberg electrons to be located near the target nucleus. This scaling relationship improves at higher photon energies (greater than 100 eV above the double-escape threshold). Another feature of the partial cross section ratios is the appearance of a peak value at energies of several eV above threshold for  $n = 4-6$ . This feature is also seen in the experimental data. Peaks are observed in our  $\text{He}^+(n)$  *absolute* cross sections for  $n \geq 5$ .

Partial cross sections calculated for  $\text{H}^-$  were found to exhibit many of the same features as in helium. A box of roughly twice the radius used in our helium calculations is required to accurately describe  $\text{H}^-$  PIE, since hydrogen wavefunctions extend roughly twice as far as those of  $\text{He}^+$ . In contrast to helium, the  $n = 2$  partial cross section for  $\text{H}^-$  is about two-thirds as large as the  $n = 1$  cross section. This is primarily a reflection of the relatively large overlap of the  $\text{H}^-$  ground state with the  $n = 2$  target eigenstates. Our  $n = 1$  and  $n = 2$  cross sections agree well with the theoretical values of Broad and Reinhardt [18]. Peaks occur in our  $n = 5$  and  $n = 6$  branching ratios at energies above the double-escape threshold, and these partial cross sections are also observed to satisfy a  $1/n^3$  scaling law for  $n \geq 3$ .

Our present eigenchannel  $R$ -matrix approach neglects the exchange of angular momentum and energy between the electrons in the region outside of the reaction volume. As such, this approach does not represent all of the details of a scattering process that are sensitive to long-range forces other than a screened Coulomb potential. Our approximation for the wavefunction outside of the reaction volume neglects the effect of long-range multipole interactions between the outer electron and the remaining fragment. The effect of neglecting the long-range dipole interaction can be understood by examining the form of this interaction as outlined by Gailitis and Damburg [19]. The dipole interaction mixes states with the same specified principal quantum number but different angular momentum values. Our method is therefore able to properly predict the correct cross sections for PIE to the  $n = 2$  state, but might not be expected to give accurate amplitudes of the individual Gailitis–Damburg eigenstates (eigenstates of the dipole matrix with basis elements  $|2s\epsilon p\rangle$ ,  $|2p\epsilon s\rangle$  and  $|2p\epsilon d\rangle$ ). A previous study [20] showed that there are no major difficulties in including the long-range dipole interaction in an eigenchannel  $R$ -matrix approach. It is possible that these long-range correlations could still play an important role in determining the angular distribution of the photoelectron; this issue remains to be tested.

In conclusion, we have studied the role of electron–electron interactions in PIE processes. Although PIE has not received as much attention as double escape, this process represents an alternative and equally informative probe of electron correlations. Our study indicates that the use of a basis set restricted to a very small region in configuration space is sufficient for describing excitation to high- $n$  states. This is a surprising result, as it was previously thought that long-range correlations played a significant role in these processes. Discrete channel expansions can therefore be applied efficiently to a broader class of problems than was previously thought possible.

This work was supported in part by the National Science Foundation. We gratefully acknowledge the allocation of resources at the National Center for Supercomputer Applications at the University of Illinois, IL.

## References

- [1] Wehlitz R *et al* 1997 *J. Phys. B: At. Mol. Opt. Phys.* **30** L51
- [2] Callaway J 1982 *Phys. Rev. A* **26** 199  
Callaway J 1988 *Phys. Rev. A* **37** 3692  
Scholz T, Scott M P and Burke P G 1988 *J. Phys. B: At. Mol. Opt. Phys.* **21** L139  
Bray I and Stelbovics A T 1992 *Phys. Rev. A* **46** 6995
- [3] Bray I, McCarthy I E, Wigley J and Stelbovics A T 1993 *J. Phys. B: At. Mol. Opt. Phys.* **26** L831
- [4] Fursa D V and Bray I 1995 *Phys. Rev. A* **52** 1279
- [5] Bray I and Stelbovics A T 1992 *Phys. Rev. A* **46** 6995  
Bray I and Stelbovics A T 1995 *Adv. At. Mol. Phys.* **35** 209
- [6] Burke P G, Noble C J and Scott M P 1987 *Proc. R. Soc. A* **410** 289  
Bartschat K, Hudson E T, Scott M P, Burke P G and Burke V M 1996 *J. Phys. B: At. Mol. Opt. Phys.* **29** 115
- [7] Burke P G and Smith K 1962 *Rev. Mod. Phys.* **34** 458
- [8] Tang J Z, Watanabe S and Matsuzawa M 1992 *Phys. Rev. A* **46** 2437  
Tang J Z and Shimamura I 1995 *Phys. Rev. A* **52** R3413
- [9] Aymar M, Greene C H and Luc-Koenig E 1996 *Rev. Mod. Phys.* **68** 1015
- [10] Meyer K W and Greene C H 1994 *Phys. Rev. A* **50** R3573
- [11] Meyer K W, Greene C H and Esry B D 1997 *Phys. Rev. Lett.* **78** 4902
- [12] Berakdar J and Briggs J S 1994 *Phys. Rev. Lett.* **72** 3799
- [13] Wannier G 1953 *Phys. Rev.* **90** 817  
Peterkop R 1971 *J. Phys. B: At. Mol. Phys.* **4** 513  
Rau A R P 1971 *Phys. Rev. A* **4** 207
- [14] Wehlitz R, Heiser F, Hemmers O, Langer B, Menzel A and Becker U 1991 *Phys. Rev. Lett.* **67** 3764
- [15] Meyer K W, Greene C H and Bray I 1995 *Phys. Rev. A* **52** 1334
- [16] Samson J A R, He Z X, Yin L and Haddad G N 1994 *J. Phys. B: At. Mol. Opt. Phys.* **27** 887
- [17] Dalgarno A and Stewart A L 1960 *Proc. Phys. Soc.* **76** 49  
Aberg T 1970 *Phys. Rev. A* **2** 1726
- [18] Broad J T and Reinhardt W P 1976 *Phys. Rev. A* **14** 2159
- [19] Gailitis M and Damburg R 1963 *Proc. Phys. Soc.* **82** 192
- [20] Sadeghpour H R and Cavagnero M 1993 *J. Phys. B: At. Mol. Opt. Phys.* **26** L271